

Multiple Coupled Circuit Modeling of Induction Machines

Xiaogang Luo, Yuefeng Liao, *Member, IEEE*, Hamid A. Toliyat, *Member, IEEE*, Ahmed El-Antably, and Thomas A. Lipo, *Fellow, IEEE*

Abstract—A new multiple coupled circuit model is presented for simulation of induction machines with both arbitrary winding layout and/or unbalanced operating conditions. The model is derived by means of winding functions. No symmetry is assumed. The parameters of the model are calculated directly from the geometry and winding layout of the machine. The behavior of an induction machine during starting is simulated using this model. The results are shown to be in good agreement with the solution obtained by a conventional $d - q$ model for symmetric conditions. The new model is then extended to the solution of a wide variety of fault conditions such as broken bars and end rings and open or short circuited motor coils.

I. INTRODUCTION

WHILE the literature on the analysis of induction machinery is rich and extensive, suitable models to analyze the transients involving multiple internal fault conditions within the motor itself have yet to appear. It is well known that the conventional $d - q$ model of an ac machine is based on the assumption that the stator windings are sinusoidally distributed, so that this model is not suitable for study of a general machine with arbitrarily connected windings. It appears, however, that a model based on the basic geometry and winding layout of an arbitrary n phase machine would be much more suitable for a general purpose, time domain simulation of an ac machine [1]. In such a model, parameters (particularly the mutual inductances between stator and rotor windings) are considered to be time-varying and can be evaluated (or looked up) in real time, while secondary parameters such as end-turn effect, leakage inductances are precalculated and treated as constants. A detailed depiction of the procedure needed to implement such a general purpose model together with simulation results of the completed model are the subjects of this paper.

II. SYSTEM EQUATIONS

Consider, for generality, an induction machine having m stator circuits and n rotor bars. (Note that there are assumed

Paper IPCSD 94-77, approved by the Electric Machines Committee of the IEEE Industry Applications Society for presentation at the 1993 IEEE Industry Applications Society Annual Meeting, Toronto, Ontario, Canada, October 3-8. Manuscript released for publication September 9, 1994.

X. Luo and T. Lipo are with the Department of Electrical & Computer Engineering, University of Wisconsin, Madison, WI 53706-1691 USA.

Y. Liao is with General Electric Company, Corporate Research & Development, Schenectady, NY 12301 USA.

H. A. Toliyat is with the Electrical Engineering Department, Texas A&M University, College Station, TX 77843-3128 USA.

A. El-Antably is with Delco Remy Division of General Motors, Anderson, IN 46018-2439 USA.

IEEE Log Number 9408187.

to be m stator circuits instead of m stator phases). The cage can be viewed as n identical and equally spaced rotor loops. Then the equations for the induction machine can be written in vector-matrix form as

$$V_s = R_s I_s + \frac{d\Lambda_s}{dt} \quad (1)$$

$$V_r = R_r I_r + \frac{d\Lambda_r}{dt} \quad (2)$$

$$\Lambda_s = L_{ss} I_s + L_{sr} I_r \quad (3)$$

$$\Lambda_r = L_{sr}^T I_s + L_{rr} I_r \quad (4)$$

where the matrix L_{sr}^T is the transpose of matrix L_{sr} , and

$$I_s = [i_{s1} \ i_{s2} \ \cdots \ i_{sm}]^T \quad (5)$$

$$I_r = [i_{r1} \ i_{r2} \ \cdots \ i_{rn}]^T \quad (6)$$

$$V_s = [v_{s1} \ v_{s2} \ \cdots \ v_{sm}]^T \quad (7)$$

In the case of a cage rotor, $V_r = [0]$. Note that with this formulation, the currents in the m stator circuits and n rotor bars are assumed as independent. The circuits can be later connected in any fashion whatsoever to form the stator winding phases and the rotor bar/end ring configuration to be investigated.

The torque and mechanical equations for the machine are

$$T_e = I_s^T \frac{\partial L_{sr}}{\partial \theta} I_r \quad (8)$$

$$\frac{d\omega}{dt} = \frac{1}{J} (T_e - T_L) \quad (9)$$

$$\frac{d\theta}{dt} = \omega \quad (10)$$

where θ is the mechanical angle, ω is mechanical speed, T_L is load torque, and J is the inertia of the rotor.

III. CALCULATION OF INDUCTANCES

It is apparent that the calculation of all the machine inductances as defined by the inductance matrices in the previous section is the key to the successful simulation of an induction machine. These machine inductances are conveniently calculated by means of winding functions. This method assumes no symmetry in the placement of any motor coil in the slots. According to winding function theory, the mutual inductance between any two windings "i" and "j" in any electric machine can be computed by the equation (assume that permeance of iron is infinite) [2]:

$$L_{ij}(\varphi) = \mu_0 Lr \int_0^{2\pi} g^{-1}(\varphi, \theta) N_i(\varphi, \theta) N_j(\varphi, \theta) d\theta \quad (11)$$

where φ is the angular position of the rotor with respect to some stator reference, θ is a particular angular position along the stator inner surface, $g^{-1}(\varphi, \theta)$ is termed the inverse gap function which becomes $1/g$ due to the assumption of uniform air gap. The quantity L is the length of stack and r is the average radius of air gap. The term $N_i(\varphi, \theta)$ is called the winding function and represents, in effect, the MMF distribution along the air gap for a unit current flowing in winding i . The self-inductance terms can be calculated by merely setting $i = j$. Equation (11) is the general expression of inductances between any two windings in an electric machine. Since our goal is to deal with arbitrary distribution of windings, it is convenient to employ another form of this equation to complete the task of calculating the inductances of the machine.

From winding function theory it is also known that the MMF at any θ of the air gap produced by current i_A flowing in coil A is

$$F_A(\theta) = N_A(\theta) \cdot i_A. \quad (12)$$

Consider now a second coil B having n_B turns (where $n_B(\theta)$ is the winding distribution of coil B) as shown in Fig. 1. It is desired to calculate the flux linking this coil due to current flowing in coil A. For this purpose, the flux in the gap is related to the MMF by

$$\Phi = F \cdot P \quad (13)$$

where P is the permeance of the air gap of cross-section A and air gap length g , and F is the MMF drop across the length g . Referring to Fig. 1 the differential flux across the air gap from rotor to stator through cross section $(r \cdot d\theta) \cdot L$ is

$$d\Phi = F_A(\theta) \mu_0 r L \frac{d\theta}{g}. \quad (14)$$

Consider now the flux linking coil B. The differential flux linkage of coil B now is

$$d\Lambda_{BA} = \frac{\mu_0 r L}{g} i_A n_B(\theta) N_A(\theta) d\theta. \quad (15)$$

The gross flux linkage in winding B is

$$\Lambda_{BA} = \frac{\mu_0 r L}{g} i_A \int_{\theta_{B1}}^{\theta_{B2}} n_B(\theta) N_A(\theta) d\theta. \quad (16)$$

Therefore the inductance between coil A and coil B is

$$L_{BA} = \frac{\mu_0 r L}{g} \int_{\theta_{B1}}^{\theta_{B2}} n_B(\theta) N_A(\theta) d\theta. \quad (17)$$

Equation (17) is now ready for calculating inductances based on the coil geometry. The following is an example of how this equation is used to calculate inductances between stator coils and rotor loops.

Referring to Fig. 2 (assuming that the pitch of any coil in the stator is greater than that of rotor slot), there are five different relative positions between any stator coil and rotor loop. Because a coil is simply a concentric winding, the

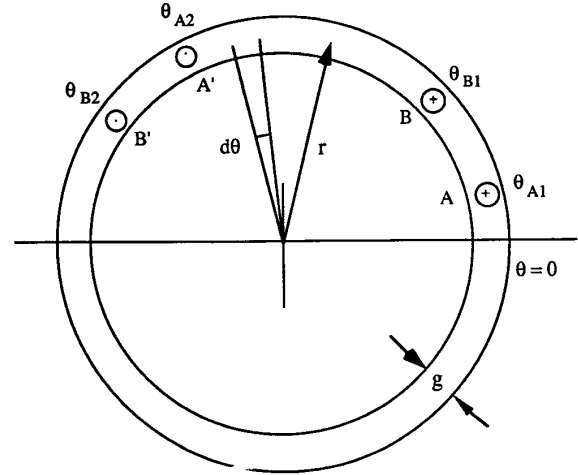


Fig. 1. Spatial positions of coil A and coil B.

winding function of coil i is

$$\begin{aligned} N_i(\theta) &= w_i - w_i \frac{\alpha_i}{2\pi} & \theta_{i1} \leq \theta \leq \theta_{i2} \\ N_i(\theta) &= -w_i \frac{\alpha_i}{2\pi} & \text{the rest of } \theta \end{aligned} \quad (18)$$

and winding distribution of loop j is

$$\begin{aligned} n_j(\theta) &= 1 & \theta_{j1} \leq \theta \leq \theta_{j2} \\ n_j(\theta) &= 0 & \text{the rest of } \theta \end{aligned} \quad (19)$$

where $\alpha_i = \theta_{i2} - \theta_{i1}$ is the pitch of coil i , and w_i is the number of turns of coil i .

From (17) and Fig. 2 the mutual inductances between stator coils and rotor loops can be written as follows:

a) For $\theta_{j1} < \theta_{j2} \leq \theta_{i1} < \theta_{i2}$ and $\theta_{i1} < \theta_{i2} \leq \theta_{j1} < \theta_{j2}$

$$L_{cirj} = L_{rjci} = \frac{\mu_0 r L w_i}{g} \left(-\frac{\alpha_i \alpha_r}{2\pi} \right) \quad (20)$$

where $\alpha_r = \theta_{j2} - \theta_{j1}$ is the pitch of rotor teeth.

b) For $\theta_{j1} < \theta_{i1} < \theta_{j2} < \theta_{i2}$

$$L_{cirj} = L_{rjci} = \frac{\mu_0 r L w_i}{g} \left[(\theta_{j2} - \theta_{i1}) - \frac{\alpha_i \alpha_r}{2\pi} \right]. \quad (21)$$

c) For $\theta_{i1} < \theta_{j1} < \theta_{i2} < \theta_{j2}$

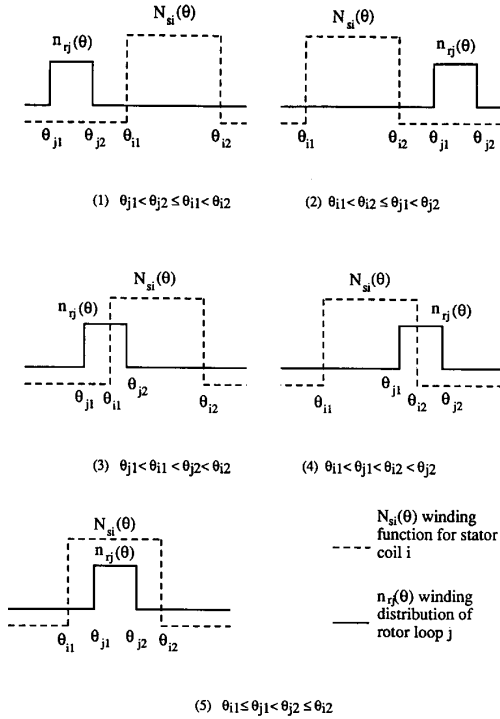
$$L_{cirj} = L_{rjci} = \frac{\mu_0 r L w_i}{g} \left[(\theta_{i2} - \theta_{j1}) - \frac{\alpha_i \alpha_r}{2\pi} \right]. \quad (22)$$

d) For $\theta_{i1} \leq \theta_{j1} < \theta_{j2} \leq \theta_{i2}$

$$L_{cirj} = L_{rjci} = \frac{\mu_0 r L w_i}{g} \left(\alpha_r - \frac{\alpha_i \alpha_r}{2\pi} \right). \quad (23)$$

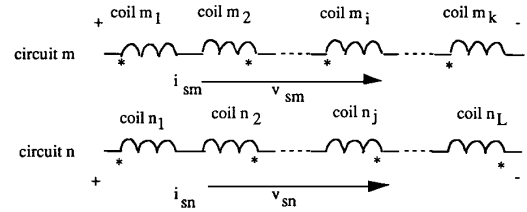
In the same manner the inductances between all stator coils, between rotor loops can be calculated.

The next step is to calculate the inductances between stator circuits, and between stator circuits and rotor loops based on the inductances already obtained for stator coils. In the general


 Fig. 2. Five different positions between stator coil i and rotor loop j .

case a circuit is composed of several coils. Fig. 3 shows two arbitrarily connected circuits m and n . Circuit m and circuit n have k and l coils respectively. From the connection and linear circuit theory, the voltage equation for circuit m is

$$\begin{aligned}
 v_{sm} = & (L_{m1m1} - L_{m1m2} + \dots + L_{m1mi} \\
 & + \dots + L_{m1mk}) \frac{di_{sm}}{dt} \\
 & + (-L_{m2m1} + L_{m2m2} + \dots - L_{m2mi} \\
 & + \dots - L_{m2mk}) \frac{di_{sm}}{dt} \\
 & + \dots + (L_{mim1} - L_{mim2} + \dots + L_{mimi} \\
 & + \dots + L_{mimk}) \frac{di_{sm}}{dt} \\
 & + \dots + (L_{mkm1} - L_{mkm2} + \dots + L_{mkmi} \\
 & + \dots + L_{mkmk}) \frac{di_{sm}}{dt} \\
 & + (L_{m1n1} - L_{m1n2} + \dots - L_{m1nj} \\
 & + \dots - L_{m1nl}) \frac{di_{sn}}{dt} \\
 & + (-L_{m2n1} + L_{m2n2} + \dots + L_{m2nj} \\
 & + \dots + L_{m2nl}) \frac{di_{sn}}{dt} \\
 & + \dots + (L_{min1} - L_{min2} + \dots - L_{minj} \\
 & + \dots - L_{minl}) \frac{di_{sn}}{dt} \\
 & + \dots + (L_{mkn1} - L_{mkn2} + \dots - L_{mknj} \\
 & + \dots - L_{mknl}) \frac{di_{sn}}{dt}.
 \end{aligned} \quad (24)$$


 Fig. 3. Connections of circuit m and n .

Equation (24) can be written as

$$v_{sm} = L_{smm} \frac{di_{sm}}{dt} + L_{smn} \frac{di_{sn}}{dt}. \quad (25)$$

From (24) it is clear that the self inductance of circuit m is given by

$$\begin{aligned}
 L_{smm} = & (L_{m1m1} - L_{m1m2} + \dots \\
 & + L_{m1mi} + \dots + L_{m1mk}) \\
 & + (-L_{m2m1} + L_{m2m2} + \dots \\
 & - L_{m2mi} + \dots - L_{m2mk}) \\
 & + \dots + (L_{mim1} - L_{mim2} + \dots \\
 & + L_{mimi} + \dots + L_{mimk}) \\
 & + \dots + (L_{mkm1} - L_{mkm2} + \dots \\
 & + L_{mkmi} + \dots + L_{mkmk})
 \end{aligned} \quad (26)$$

and the mutual inductance between circuit m and circuit n is given by

$$\begin{aligned}
 L_{smn} = & (L_{m1n1} - L_{m1n2} + \dots \\
 & - L_{m1nj} + \dots - L_{m1nl}) \\
 & + (-L_{m2n1} + L_{m2n2} + \dots \\
 & + L_{m2nj} + \dots + L_{m2nl}) \\
 & + \dots + (L_{min1} - L_{min2} + \dots \\
 & - L_{minj} + \dots - L_{minl}) \\
 & + \dots + (L_{mkn1} - L_{mkn2} + \dots \\
 & - L_{mknj} + \dots - L_{mknl}).
 \end{aligned} \quad (27)$$

In general, the mutual inductance between any circuit m and circuit n can be written as

$$L_{smn} = \sum_{i=1}^k \sum_{j=1}^l \pm L_{minj} \quad (28)$$

where L_{minj} is the mutual inductance between coil mi and coil nj . The sign before L_{minj} is determined according to the manner of connection of these coils. When $m = n$, (28) yields the self inductance of circuit m .

In the simulation program an input matrix is needed to describe the connection of stator circuits in terms of coils for calculating the circuit inductances using (28), so that the sign before L_{minj} can be determined. Finally the leakage inductances calculated from design data must be added to form the corresponding circuit self inductances [3].

All the inductances except the mutual inductances between stator and rotor are rotor position independent because of the round stator and rotor structure. Although it is possible

to calculate these inductances at any position during the simulation iteration loop, the task typically consumes too much calculation time. The solution to this problem is simple interpolation. Discrete curves of inductance versus rotor angular position are calculated outside the iteration loop. Inside the loop the inductances are obtained by a simple look-up table method, i.e., by interpolation. The accuracy of the interpolation is crucial to the success of the simulation because a small error in the mutual inductances can be reflected as additional stator and rotor winding leakage inductances, or the decrease of mutual coupling between stator and rotor windings.

For an accurate interpolation, the discretization of the inductance curve is important. The inductance variation curve is continuous, piecewise linear function, and the derivative of it is piecewise continuous function due to the nature of winding function method. From Fig. 2 one can determine that when any two stator coil side and rotor loop side align, the curve reaches its turning point, i.e., its derivative changes abruptly. Denoting the stator slot pitch τ_s and rotor slot pitch τ_r , and defining the step (angle increment) as $\Delta\theta$, the number of steps or angle increments must meet the following equations which guarantee that all the turning points of the curve fall in the discretization points

$$\frac{\tau_s}{\Delta\theta} = \text{integer} \quad (29)$$

$$\frac{\tau_r}{\Delta\theta} = \text{integer}. \quad (30)$$

When the number of steps over 2π is chosen to be the least common product of the number of stator slots and the number of rotor slots, the above requirements are met. Under these circumstances the variation of the inductances between any adjacent two point is linear, so that linear interpolation provides fast, accurate results.

IV. LINE-TO-LINE MODEL

Unfortunately, the above model is still not suitable for a general purpose simulation because it requires stator phase voltages as inputs, whereas usually what are known are the line-to-line voltages. Although under symmetrical, balanced operation it is not difficult to obtain the phase voltages from line-to-line voltages, the problem is much more difficult for the case of a general unbalanced connection. Hence, there is a need for establishing a model which can employ line-to-line voltages as inputs.

The circuits can now be connected to form the machine stator winding configuration. While the approach is general, it is useful to consider the particular case of a three phase circuit case as shown in Fig. 4 [1], [4]. From this sketch one can write the stator equations as follows:

$$V_s = \begin{bmatrix} R_a & 0 & 0 \\ 0 & R_b & 0 \\ 0 & 0 & R_c \end{bmatrix} I_s + \begin{bmatrix} \frac{d\Lambda_{sa}}{dt} \\ \frac{d\Lambda_{sb}}{dt} \\ \frac{d\Lambda_{sc}}{dt} \end{bmatrix} \quad (31)$$

$$\Lambda_s = \begin{bmatrix} L_{saa} & L_{sab} & L_{sac} \\ L_{sba} & L_{sbb} & L_{sbc} \\ L_{sca} & L_{scb} & L_{scc} \end{bmatrix} I_s + \begin{bmatrix} L_{sar} \\ L_{sbr} \\ L_{scr} \end{bmatrix} I_r \quad (32)$$

where L_{sar} , L_{sbr} , and L_{scr} are 1 by n row vectors.

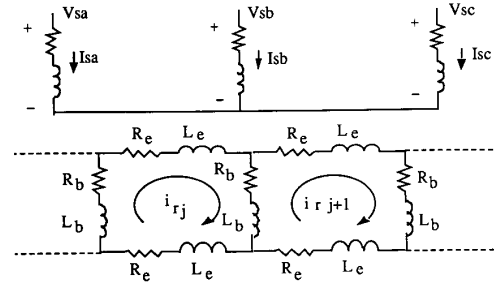


Fig. 4. Three phase stator windings and rotor loop windings adapted from [1].

Subtracting each row in (31) and (32) by the following row, one obtains

$$\begin{aligned} V_{st-l} &= \begin{bmatrix} R_a & -R_b & 0 \\ 0 & R_b & -R_c \\ -R_a & 0 & R_c \end{bmatrix} I_s + \begin{bmatrix} \frac{d\Lambda_{sa}}{dt} - \frac{d\Lambda_{sb}}{dt} \\ \frac{d\Lambda_{sb}}{dt} - \frac{d\Lambda_{sc}}{dt} \\ \frac{d\Lambda_{sc}}{dt} - \frac{d\Lambda_{sa}}{dt} \end{bmatrix} \\ &= \begin{bmatrix} R_a & -R_b & 0 \\ 0 & R_b & -R_c \\ -R_a & 0 & R_c \end{bmatrix} I_s + \frac{d\Lambda_{st-l}}{dt} \quad (33) \\ \Lambda_{st-l} &= \begin{bmatrix} \Lambda_{sa} - \Lambda_{sb} \\ \Lambda_{sb} - \Lambda_{sc} \\ \Lambda_{sc} - \Lambda_{sa} \end{bmatrix} \\ &= \begin{bmatrix} L_{saa} - L_{sba} & L_{sab} - L_{sbb} & L_{sac} - L_{sbc} \\ L_{sba} - L_{sca} & L_{sbb} - L_{scb} & L_{sbc} - L_{scc} \\ L_{sca} - L_{saa} & L_{scb} - L_{sab} & L_{scc} - L_{sac} \end{bmatrix} \\ &\quad \cdot I_s + \begin{bmatrix} L_{sar} - L_{sbr} \\ L_{sbr} - L_{scr} \\ L_{scr} - L_{sar} \end{bmatrix} I_r. \quad (34) \end{aligned}$$

No matter if the phases are balanced, symmetrical and identical or not, if the stator windings are Y connected, the sum of stator currents is zero. Hence, (34) can be written as

$$\begin{aligned} &\begin{bmatrix} \Lambda_{sa} - \Lambda_{sb} \\ \Lambda_{sb} - \Lambda_{sc} \\ 0 \end{bmatrix} \\ &= \begin{bmatrix} L_{saa} - L_{sba} & L_{sab} - L_{sbb} & L_{sac} - L_{sbc} \\ L_{sba} - L_{sca} & L_{sbb} - L_{scb} & L_{sbc} - L_{scc} \\ 1 & 1 & 1 \end{bmatrix} I_s \\ &\quad + \begin{bmatrix} L_{sar} - L_{sbr} \\ L_{sbr} - L_{scr} \\ 0 \end{bmatrix} I_r. \quad (35) \end{aligned}$$

Equations (2), (4), (8)–(10), (33), and (35) form the line-to-line model useful for purposes of simulation. Although three stator phases have been considered here explicitly, one can derive a similar model for an arbitrary number of stator circuits following the same procedure. Also, in the same fashion one can derive the models for any number of phases and circuits. Note that because the rotor windings are short circuited, so that there is no need for modification of the equations on the rotor side.

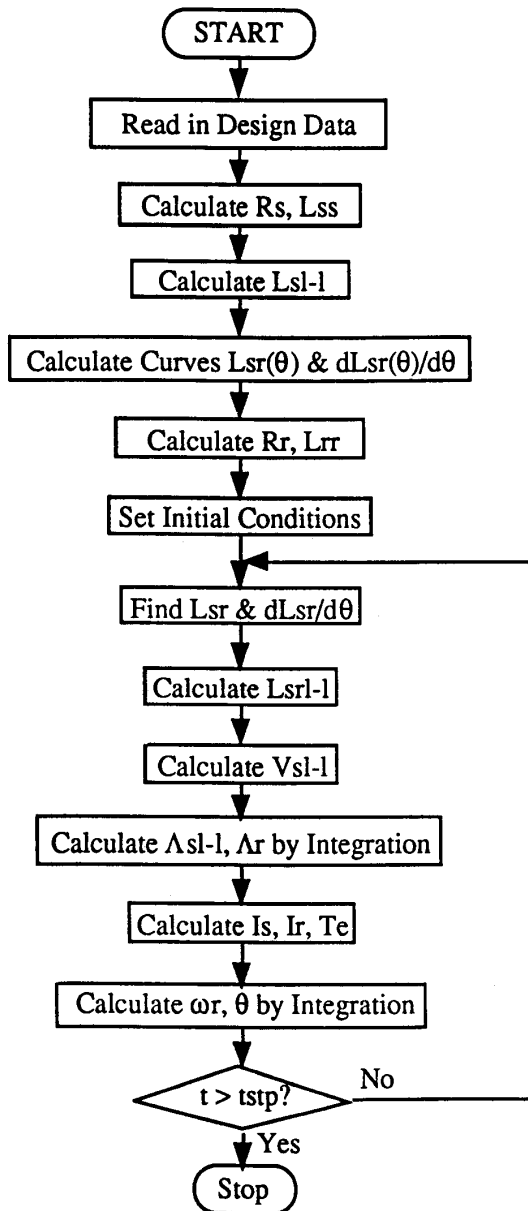


Fig. 5. Flow chart of simulation program.

V. SIMULATION

Using the model derived, a simulation study has been conducted on a typical induction machine. Fig. 5 is the flow chart for the simulation program. The method described previously is used to calculate the inductances. The resistances are calculated in the conventional manner [3]. Note that this is simply a linear model and accurate values of parameters are difficult to obtain when saturation occurs.

For purposes of comparison the model is first used to simulate the acceleration transient of a symmetrical three-phase machine from rest under sinusoidal voltage excitation and the results are shown in Fig. 6. The quantity I_{ckt1} in

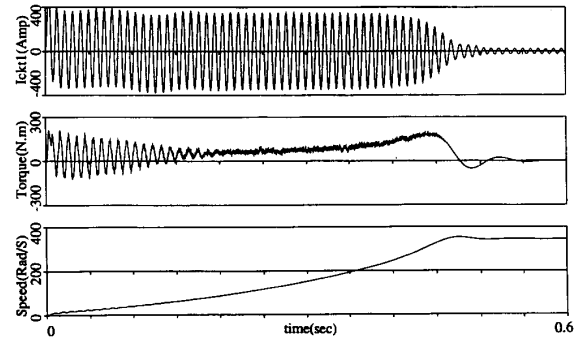


Fig. 6. Acceleration transient using new model under sinusoidal voltage excitation.

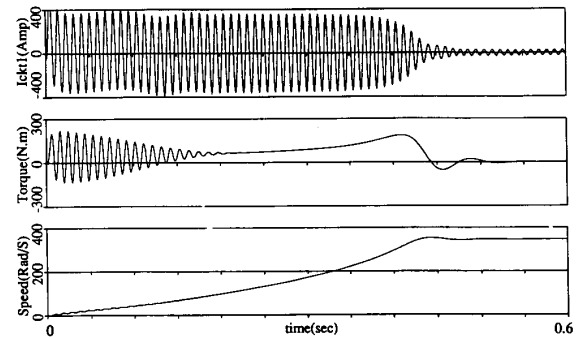


Fig. 7. Acceleration transient using conventional $d-q$ model with sinusoidal voltage excitation.

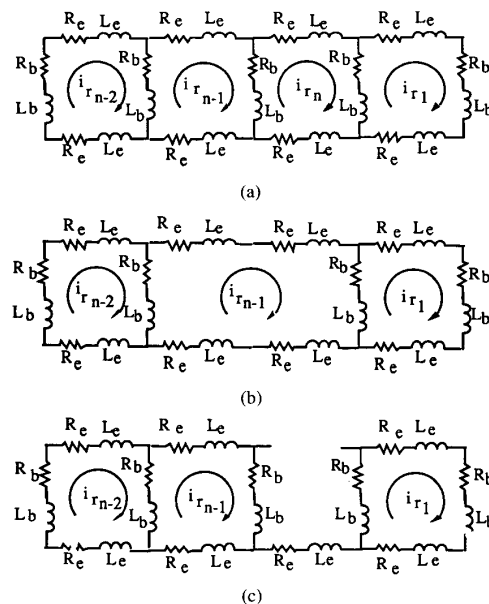


Fig. 8. Fault conditions of rotor. (a) Normal. (b) Last bar broken. (c) Last end ring segment broken.

Figs. 6, 7, 9, and 10 denotes the current of first circuit of phase A. In Fig. 7 the same machine is simulated using the

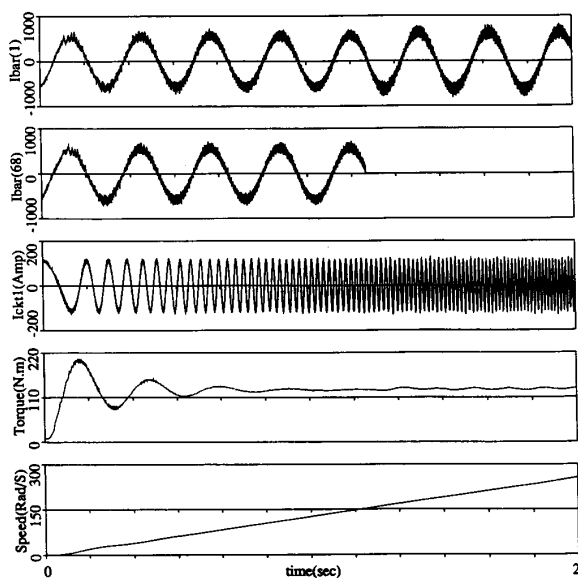


Fig. 9. Acceleration transient under CRPWM excitation wherein a bar broken fault occurs. $I_{bar}(n)$ is the current of n th bar.

conventional $d - q$ model under the same conditions for comparison. Comparison of the two simulation traces shows very good correlation. The slight deviation appears to be caused by the harmonic effects created by the simulation of each separate winding circuit. The effects of harmonics caused by these nonsinusoidal distribution of the windings are completely represented by winding function theory.

The model which has been developed can also be used with simulation techniques to solve nearly any asymmetrical conditions including broken bars, broken end ring segments, stator winding circuit open circuits, and circuit terminal to terminal short circuit faults. The open circuit faults are assumed to occur when the relevant current reaches zero because of the existence of inductances in all current paths.

Fig. 8 shows the circuit presentation of a broken bar and a broken end ring segment faults. Though we assume here that bar n or end ring segment n is broken for the convenience of simulation, it makes no difference if any other bar or end ring segment is selected because of the identical nature of the rotor loops. In the case of the broken bar, it is apparent from the theory that all parameters related to the loop $n-1$ must change, while the equation remains the same except that the equation related to loop n is dropped. Inductances related to the fault bar are recalculated when fault occurs. Fig. 9 shows the simulation results. Since the number of bars of the machine is quite large (68 bars), the broken bar does not have a significant effect on the behavior of the machine.

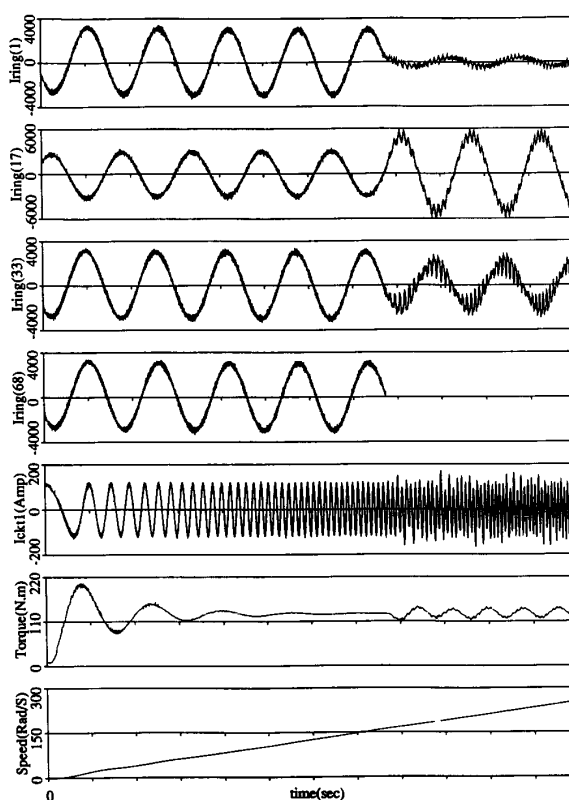


Fig. 10. Acceleration transient under CRPWM excitation in which an end ring segment broken fault occurs. $I_{ring}(n)$ is the current of n th end ring segment.

In the case of a broken end ring segment shown in Fig. 8(c), it can be seen that there is no change in parameters except for R_e and L_e of end ring segment n . However, the equations related to loop 1 and $n-1$ must be modified and the equation related to loop n is dropped. Further observation leads to the conclusion that as long as loop current i_n is forced to be zero, it has no influence on any other loop and circuit. Hence, in the simulation it is sufficient to set the current to be zero to solve the problem. The simulation results are shown in Fig. 10. The effects of broken end ring segment can be observed to have a more significant affect on the torque than bar broken case. All the loop currents are substantially affected as well as stator currents.

Fig. 11 shows two fault conditions of stator windings. In Fig. 11(a) it is shown that one of the four parallel circuits of one of the phase windings is open circuited and the simulation results are shown in Fig. 12. It can be seen that one circuit open circuited causes substantial unbalanced operation but is not so significant as the case when the entire phase is open

$R_s = 9.737e-3 \Omega$	$R_r = 5.639e-3 \Omega$	$L_{sl} = 2.685e-5 \text{ H}$	$L_{rl} = 6.376e-5 \text{ H}$
$L_m = 1.306e-3 \text{ H}$	Y connection	4 circuits/phase	$V_{l-l(rms)} = 110 \text{ V}$
$f = 110 \text{ Hz}$	$J = 0.1 \text{ kgm}^2$	CRPWM carrier frequency = 5 kHz	

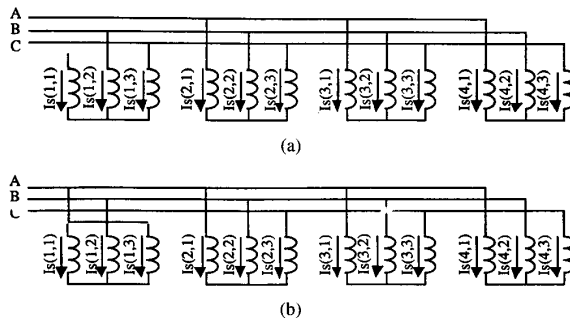


Fig. 11. Stator winding connection and fault conditions.

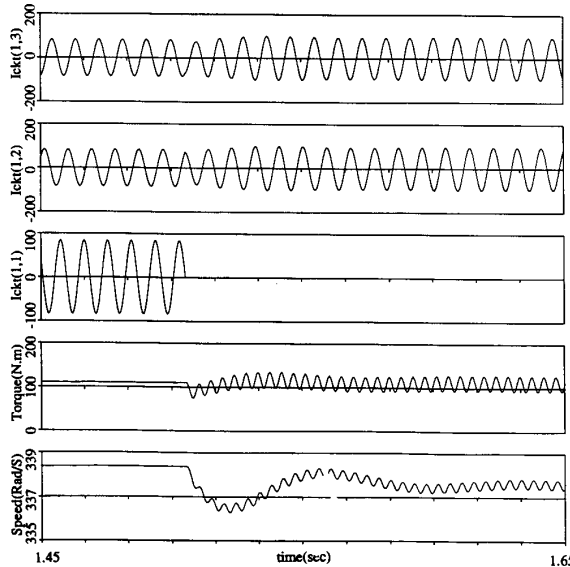


Fig. 12. A sudden open circuit of one of four parallel circuits making up one of the three stator phases.

circuited. Finally, a line-to-line short circuit fault which was depicted in Fig. 11(b) was simulated and the results are shown in Fig. 13. In this case, one of the four circuits of one phase of the machine is shorted to corresponding circuit of another phase. A large pulsation in torque is observed followed by a continual double frequency torque pulsation.

VI. CONCLUSION

A new approach to induction machine modeling has been introduced in this paper. The model is based directly on the geometry of the induction machine and the physical layout of all windings. Calculation of inductances is further carried out on coil-by-coil basis. For the general case where the phase voltages are difficult to obtain, the line to line model has been derived. This model only needs line to line voltages as excitation, so it can be readily applied for analysis of arbitrary unbalanced operation of an induction machine. Simulation results have confirmed the validity of the model. Because the coupled circuit model takes into account arbitrary winding distributions, it should prove very useful for fault analysis

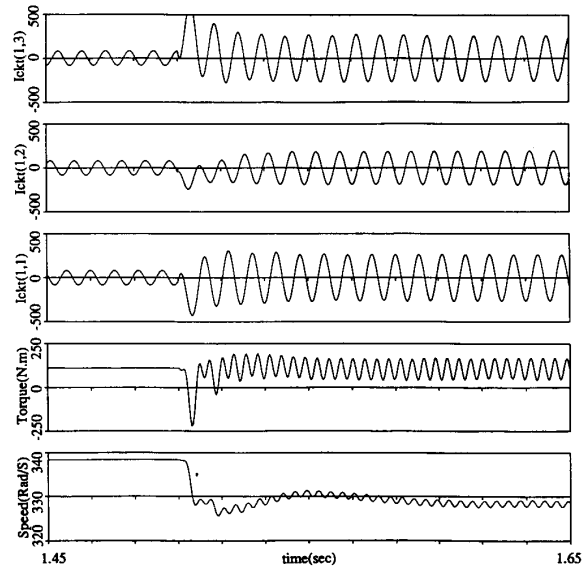


Fig. 13. A sudden line-to-line short circuit of two circuits.

wherein the fault occurs within the winding itself. A general purpose simulation program has been developed employing this model. Several fault operations of the induction machine have been simulated to demonstrate its versatility. It has also been shown that the results are consistent with the results of the conventional method for balanced, symmetrical operation.

APPENDIX
MACHINE PARAMETERS

Machine Ratings:

114 hp 110 V 80 A/Circuit 4 Poles 220 Hz.

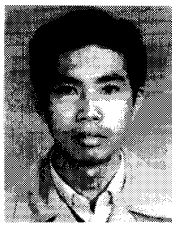
Machine Parameters: [see table at the bottom of previous page].

ACKNOWLEDGMENT

The support and encouragement of Ron Martin of Delco-Remy of GM during the course of this project is gratefully acknowledged.

REFERENCES

- [1] H. A. Toliyat, "Analysis of concentrated winding induction and reluctance machines for adjustable speed drive applications," Ph.D. thesis, Department of Electrical and Computer Engineering, University of Wisconsin, Madison, 1991.
- [2] T. A. Lipo, "Analysis and control of synchronous machines," Course Notes for ECE 511, Department of Electrical and Computer Engineering, University of Wisconsin, Madison, 1986.
- [3] ———, "AC machine design," Course Notes for ECE 713, Department of Electrical and Computer Engineering, University of Wisconsin, Madison, 1991.
- [4] H. R. Fudeh and C. M. Ong, "Modeling and analysis of induction machines containing space harmonics, Part I," *IEEE Trans. PAS*, vol. 102, no. 8, pp. 2608–2615, Aug. 1983.



Xiaogang Luo was born in Guangdong, China, in 1957. He received the M.Eng. degree from Fuzhou University, Fuzhou, China, in 1987, and the B.Eng. degree from South China University of Technology, Guangzhou, China, in 1982.

He was with the Department of Electric Power Engineering, South China University of Technology, Guangzhou, from 1985 to 1991, as a lecturer. He has been a graduate student at the University of Wisconsin, Madison, since 1991, pursuing the Ph.D. degree. His research interests are in electrical machines, machine drives, and power electronics.



Yufeng Liao (S'91-M'92) is a native of Canton, China. He received the B.S. and M.S. degrees in electrical engineering from Tsinghua University, Beijing, China, in 1983 and 1986, respectively. He received the Ph.D. in electrical engineering from the University of Wisconsin, Madison, in 1992.

He was a lecturer at South China University of Technology, Canton, from 1986 to 1988. From 1992 to 1994, he was an Engineering Specialist with Emerson Motor Technology Center, Emerson Electric Company, St. Louis, MO. He is presently an Electrical Engineer in the Corporate Research and Development Center of General Electric Company. His interests are focused mainly on new ac motor and drive system development and its applications.

Dr. Liao has published 20 papers in this area, including a second-prize paper from the IEEE Industry Applications Society in 1994, a first-prize paper from the Industrial Drives Committee at the 1993 Industry Applications Annual Meeting, and a second-prize paper from the Electric Machines Committee at the 1992 Industry Applications Annual Meeting. He is co-recipient of several U.S. patents. He serves on the Industrial Drives Committee and the Electric Machines Committee of the Industry Applications Society of the IEEE.



Hamid A. Toliyat (S'87-M'91) was born in Mashhad, Iran, in 1957. He received the B.S. degree from Sharif University of Technology, Tehran, Iran, in 1982, the M.S. degree from West Virginia University, Morgantown, in 1986, and the Ph.D. degree from the University of Wisconsin, Madison, in 1991, all in electrical engineering.

Between 1982 and 1984, he worked for power companies in Iran. While working toward the Ph.D., he was a teaching/research assistant at the University of Wisconsin, and a consultant to several industrial concerns. In 1991, he joined the faculty of Ferdowsi University, Mashhad, as an Assistant Professor of Electrical Engineering. He is currently employed by Texas A&M University, College Station, as a Visiting Assistant Professor, where he is involved in teaching and research with a multidisciplinary team, working on hybrid electric vehicles. His main research areas include converter optimized induction and synchronous reluctance machines, power electronics, power systems, and control.

Dr. Toliyat is a member of the IEEE Power Engineering Society and Sigma Xi.



Ahmed El-Antably received the B.S. degree in electrical engineering, Cairo University, Egypt, in 1968. He received the M.S. degree in control engineering and the Ph.D. degree in electrical engineering from the University of Sussex, England, in 1975 and 1980, respectively.

He worked in the oil fields pumping stations from 1968 to 1973. He was employed by Westinghouse Electric Corporation from 1980 to 1989. During this period, he was involved in the design, analysis, manufacturing, testing, and service of electric drive motor systems of the direct-current, induction, synchronous, and permanent magnet motors of many sizes for industrial, commercial, and military applications. He spent some time at Westinghouse R&D Center, designing energy-efficient synchronous reluctance machines. He also worked at control systems analysis for Westinghouse nuclear power plants. In 1989, he joined AC Delco Systems "General Motors Corporation," where he is a staff engineer in the development, design, and support of the electric drive motors for various electric propulsion systems, including the drive motor for the electric vehicle (IMPACT) program, electric hybrid shuttle buses, electric hybrid vans, and large electric drive motors for military applications. He is also responsible for developing advanced second generation drive motors for future electric propulsion applications. He has 15 publications and four patents.



Thomas A. Lipo (M'64-SM'71-F'87) is a native of Milwaukee, WI. He received the B.E.E. and M.S.E.E. degrees from Marquette University, Milwaukee, in 1962 and 1964, respectively, and the Ph.D. degree in electrical engineering from the University of Wisconsin, Madison, in 1968.

From 1969 to 1979, he was an Electrical Engineer in the Power Electronics Laboratory of Corporate Research and Development of the General Electric Company, Schenectady, NY. He became Professor of Electrical Engineering at Purdue University, West Lafayette, IN, in 1979, and in 1981, joined the University of Wisconsin, Madison, in the same capacity, and where he is presently the W. W. Grainger Professor for Power Electronics and Electrical Machines. He has been engaged in power electronics research for over 30 years.

Dr. Lipo has received 17 IEEE prize paper awards for his work, including co-recipient of the Best Paper Award in the IEEE TRANSACTIONS ON INDUSTRY APPLICATIONS in 1984. In 1986, he received the Outstanding Achievement Award from the IEEE Industry Applications Society for his contributions to the field of ac drives, and in 1990, received the William E. Newell Award of the IEEE Power Electronics Society for contributions to the field of power electronics. He served as the President of the IEEE Industry Applications Society in 1994.